Landslides and tsunamis of December 30, 2002 at Stromboli, Italy: numerical simulations

S. Tinti, A. Armigliato, A. Manucci, G. Pagnoni and F. Zaniboni

Department of Physics, Sector of Geophysics, University of Bologna, Italy

(Received August 2, 2004; accepted October 28, 2004)

ABSTRACT On December 30, 2002, a series of mass failures occurred in the north-western flank of Stromboli, more precisely in the northern part of the Sciara del Fuoco. Slides were clustered into two distinct complex episodes of failure, separated one from another by about 7 minutes. The first took place mainly underwater, the second one detached from above the sea level. The two tsunamis were generated by the main slides and attacked the Island of Stromboli. The damage was severe, especially on the northern and eastern coast of the island that stretches from Piscità to Pizzillo, where many houses were destroyed. No deaths were caused by the tsunamis since most houses were empty when the tsunamis attacked and because the few residents or tourists who happened to be there were alerted by the noise accompanying the water waves and were able to escape. The understanding of the event was not immediate and the sequence of facts could be reconstructed only by 1) examining the data acquired by the monitoring system before, during and after such occurrences, 2) carrying out bathymetric and aerophotogrammetric surveys to determine the displaced volumes, 3) performing post-event surveys to ascertain the physical effects of the tsunami on the coast, 4) interviewing eye-witnesses, 5) performing numerical simulations of the events. This study belongs to the last category of activities, since its main purpose is to contribute to the understanding of the complex physical phenomena that occurred at Stromboli. We use numerical codes to simulate the motion of the two main landslides and the generation and propagation of the ensuing tsunamis. This work, that complements previous simulations, focuses on the impact of the waves against the north-eastern coasts of Stromboli: here the computed retreat and flooding of the sea are shown to agree with the eye-witnesses accounts and with the boundary of the inundation zone that was identified during the post-tsunami surveys. The study shows that both tsunamis were powerful, and that the second one was only slightly smaller than the first, though it was produced by the failure of a mass with volume approximately one third of the first. The second tsunami occurred before the first one had concluded its life, superimposing itself on the queue of the first one.

1. Introduction

Stromboli is the northernmost island of the Aeolian archipelago, in the southern Tyrrhenian Sea (Fig. 1a), and is known to have experienced several tsunamis during its history. Tsunami catalogues [e.g. Tinti *et al*. (2004); see also the recent revision by Maramai *et al*. (2005)] indicate that at least five tsunamis have hit the Stromboli coasts (1916, 1919, 1930, 1944, 1954) in the last

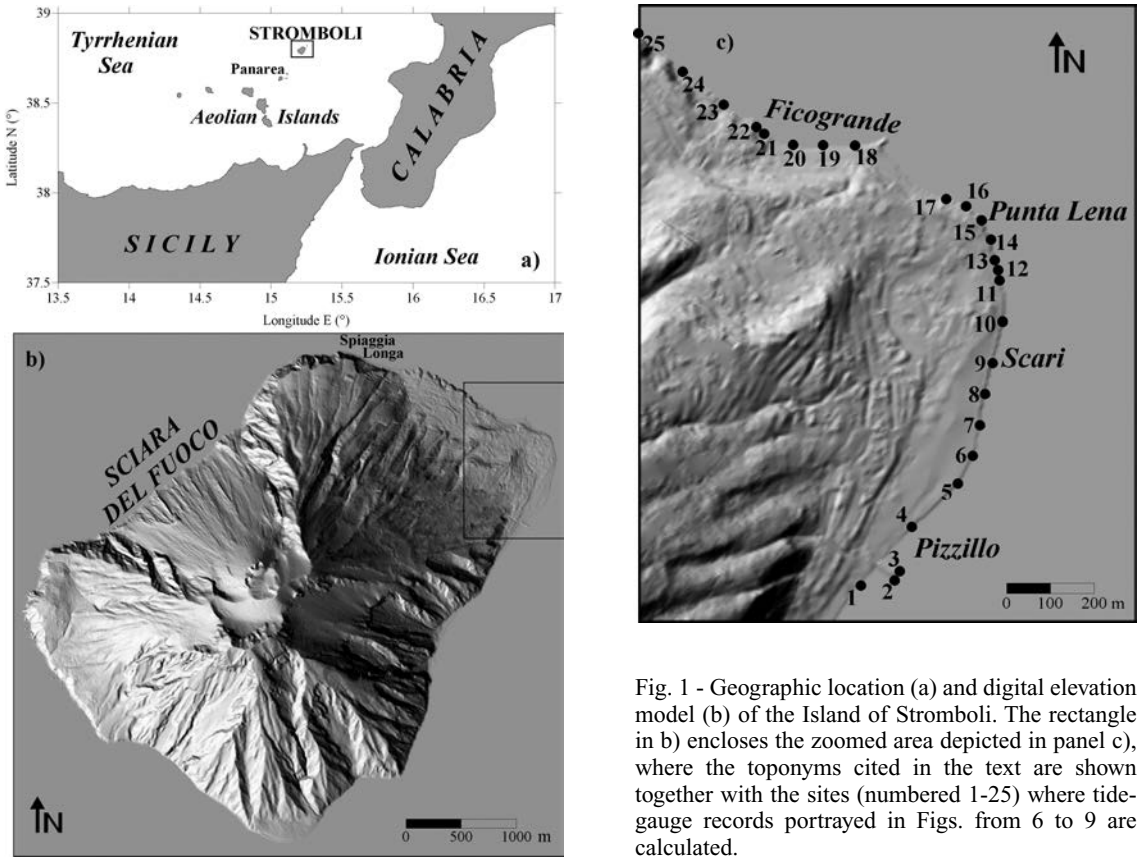

Fig. 1 - Geographic location (a) and digital elevation model (b) of the Island of Stromboli. The rectangle in b) encloses the zoomed area depicted in panel c), where the toponyms cited in the text are shown together with the sites (numbered 1-25) where tide-gauge records portrayed in Figs. from 6 to 9 are calculated.

one hundred years. Most of tsunamis that occurred in the history of the island are related to landslide and collapse phenomena taking place in correspondence with the structure known as Sciara del Fuoco (SdF) (Fig. 1b). This is an impressive scar, found on the north-western flank of the volcano, that is the remnant of the catastrophic collapse of an entire sector of the volcanic edifice that occurred in Holocene, less than 5000 years ago. The cited event was the last of four large sector collapses affecting the volcano in the last 13,000 years (Tibaldi, 2001): it involved an estimated volume of 1 km^3 of material, and probably generated a mega-tsunami that attacked not only the coasts of Stromboli (Tinti *et al*., 2000) and of the entire Aeolian archipelago, but also the whole south-eastern Tyrrhenian basin (Tinti *et al*., 2003). SdF is an intrinsically unstable structure from a gravitational point of view, both because of its very pronounced steepness and because of the continuous feeding of eruptive material provided by the persistent activity of the volcano. This gravitational instability can culminate in mass failures especially at the same time as the periodic paroxysmal crises characterising Stromboli. The last of them started in May 2002 with an increased explosive activity and evolved through different stages [see Bonaccorso *et al*. (2003) for example] till December 28, when the opening of a NE-trending eruptive fissure was observed in correspondence with the NE crater, and two lava flows were seen to propagate downslope along the SdF. The incipient mass destabilization was suggested on the following day by the appearance of transversal cracks on the SdF, and concretized on December 30 with a series of

failures starting at 13:15 local time. The peak of the sequence consisted of two main episodes, that occurred respectively at 13:15 and at 13:22. The first was a mainly submarine landslide involving the total volume of about 20×10^6 m^3, as revealed by both post-event bathymetric surveys (e.g. Chiocci *et al*., 2003a) and seismological modelling (e.g. Pino *et al*., 2004). The second main landslide, occurring 7 minutes later, was almost completely subaerial and is believed to have displaced a volume of material in the order of $4\text{-}9\times10^6$ m^3, as estimated through the comparison of pre- and post-event aerophotogrammetric data (Baldi *et al*., 2003).

The landslide phenomena were responsible for disastrous tsunami effects, that left significant traces on the environment and caused very relevant damage, especially on the northern and north-eastern portions of the island, from Spiaggia Longa to Pizzillo (Figs. 1b and 1c). One important issue is whether both the main failures or just one of them generated tsunami waves. Some authors (e.g. Pino *et al*., 2004) support the second hypothesis and suggest that only the first submarine landslide was tsunamigenic. Our position instead, is that both the submarine and the subaerial landslides produced distinct and significant tsunamis. This position is based on the critical review of the reports collected by interviewing eye-witnesses (Tinti *et al*., 2005a) and on the results of preliminary numerical simulations of both the landslides and the ensuing tsunamis (Tinti *et al*., 2005c). The present study relies on the same idea and has to be considered as a complement to the paper by Tinti *et al*. (2005c). There, different hypotheses for the geometries and the volumes of the two main landslides were taken into account, and the landslide motion and the subsequent tsunami generation, propagation and impact were computed separately for each case. Here we adopt the best models proposed by Tinti *et al*. (2005c) respectively for the submarine and the subaerial mass movements, and study the impact on the north-eastern portion of the island (Fig. 1c) of both the first tsunami on its own and the combination of the two distinct tsunamis. After summarising the available data and the numerical schemes used, we carry out the discussion on the basis of synthetic tide gauge records computed on a rich set of coastal points, as well as on the comparison of the computed sea retreat and flooding with the observed line of inundation in correspondence with the hamlet of Ficogrande (Fig. 1c).

2. Data

2.1. Instrumental data

The ground motion induced by the sequence of failures that occurred along the SdF was recorded, in particular, by a couple of seismic stations installed in Stromboli and by three broadband stations installed at Panarea, located about 20 km SW of Stromboli (Fig. 1a). The seismic records have been studied by different authors (Bonaccorso *et al*., 2003; Pino *et al*., 2004; La Rocca *et al*., 2004) in order to retrieve the onset time and the volume of material displaced by each individual failure event. The signals have also been investigated in order to identify the traces left by the impact of the tsunami waves: at the moment, there seems to be no general agreement on the results.

Only one tide-gauge record is available, namely the record of the instrument installed in the harbour of Panarea. Unfortunately, the characteristics of the instrument were not suitable to record tsunami waves properly, since it recorded a sample every five minutes and the sample itself was the average over a 40-s time window: moreover, a severe bias was introduced by the cut

of the negative waves determined by the fact that the instrument was installed just 40 cm below the lowest expected tide. Hence, this tide gauge signal can in no way help us distinguish either the number of tsunamis or their exact arrival times.

2.2. Eye-witness accounts

One of the major efforts undertaken in the weeks following the events was to interview the people that happened to be in Stromboli on December 30, 2002 and saw, with their own eyes, what occurred that day. Due to the lack, or to the ambiguity of instrumental data, the collected material, which has been critically revised by Tinti *et al*. (2005a), assumed a very important role in the reconstruction of the sequence of events, and in particular of the tsunamis. As concluded by Tinti *et al*. (2005a), the general picture resulting from the critical review of the interviews leads to state with a high level of confidence that two distinct tsunamis took place. Eye-witnesses were able to provide valuable information on the sea retreat and flooding in several places and also on the number of observed waves and on the total duration of the sea perturbation. On the other hand, it is difficult to understand which one of the two tsunamis produced the largest effects from their accounts.

2.3. Field surveys

In the days and weeks following the December 30, 2002 disastrous events, several groups of researchers were involved in a number of field surveys aimed at estimating and quantifying the impact of the tsunami waves (run-up and inundation) on the coasts of Stromboli. In particular, a team involving the authors of this paper and two researchers of INGV in Rome (Dr. Maramai and Dr. Graziani) performed three distinct post-event surveys, whose results are detailed in Tinti *et al*. (2005b). Their findings can be summarised in the following points: a) the observed effects resulted from the impact of the two distinct tsunamis that attacked within a very short time interval one from the other, and hence, it was in no way possible to discriminate between the

a) b)

Fig. 2 - Tsunami effects at Ficogrande: a) interior of a house located some tens of meters from the shoreline; b) large volcanic block brought by the tsunami waves onshore. Both pictures were taken on January 23, 2003.

effects of each individual tsunami; b) the highest run-up (10.9 m) was measured in correspondence with Spiaggia Longa, which is the surveyed coastal segment closest to the source area. Then, the run-up distribution was seen to generally decay with the distance from the source, being also related to the different topographies of the beaches, which tend to be narrow and steep in the northern sector, while the north-eastern coasts are characterised by wide and gently sloping beaches, especially in correspondence with Scari. Here the maximum horizontal penetration of 146 m was measured.

Figs. 2 to 4 illustrate some typical pictures of damage observed during the different surveys in the hamlets that will be considered later on in this paper. In particular, Fig. 2 contains two different pictures taken at Ficogrande and showing the peculiar effect produced by the sea water entering a building (Fig. 2a), with furniture and other heavy objects like a radiator torn away from the walls and heaped inside the rooms. Fig. 2b illustrates how the water waves transport heavy objects onshore, like a big volcanic boulder. Fig. 3 refers to Punta Lena, where several holiday houses are built just in front of the shoreline that along this stretch of coast is subject to very intense erosive phenomena and is protected by lines of heavy breakwater blocks. Fig. 3a shows a fence bent by the impact of the tsunami waves: by measuring the direction of the bending, we can estimate the direction of the impact of the water waves at this particular site (about 260° W). Finally, Fig. 4 illustrates a couple of examples of damage observed at Scari, with boats (Fig. 4a) and even caravans (Fig. 4b) carried onshore by the incoming water waves and thrown violently against the walls. In Fig. 4b, we have another example of a bent fence: here the bending direction suggests that the tsunami struck from the south. The comparison of the directions observed in Figs. 3a and 4b indicates that, approximately, in correspondence with Scari, two distinct tsunami fronts attacked the coastline from almost opposite directions: they are very likely two branches

a) b)

Fig. 3 - Tsunami signatures at Punta Lena. The pictures were shot on January 22, 2003: a) Fence bent by the tsunami waves in correspondence with the last house at the southern end of Punta Lena; b) typical damage produced by the water wave impact on the houses of Punta Lena built just in front of the shoreline.

a) b)

Fig. 4 - Tsunami damage observed at Scari. Both images were collected on January 13, 2003: a) boats carried onshore and thrown against house walls, uprooted vegetation and damaged buildings were typical tsunami signatures observed at Scari; b) a caravan moved away from its original location and a bent fence.

of the second tsunami (see Tinti *et al*., 2005a) radiating from the source area and travelling from there in both directions around the island: this well known phenomenon [see for example Tinti and Vannini (1995)] is due to the refraction of the tsunami waves that is caused by the large bathymetric gradients around the island.

3. Numerical simulations

3.1. Numerical models

We use two distinct models to simulate the landslides and the tsunamis.

A Lagrangian approach, with both 1D and 2D formulations, is adopted to simulate the sliding phenomena. The sliding body is partitioned into a set of blocks that are constrained to maintain their volume unaltered during the motion, while their shape is allowed to vary. The dynamics of the sliding mass is described through the acceleration of the centre of mass (Com) of each block. This can be given the general expression:

$$\vec{a}_{ij} = \vec{G}_{ij} + \vec{R}_{ij} + \vec{F}_{ij} \qquad (1)$$

where subscripts i and j indicate the i-th block and the j-th time step respectively. Term $\vec{G}_{ij}$ contains the driving gravity acceleration, bottom friction and buoyancy. $\vec{R}_{ij}$ represents the resistance to the motion opposed by the ambient fluid (for instance, free air or sea water): for each block, it acts on the upper and lateral surfaces, that is on the portions in contact with the fluid. Lastly, $\vec{F}_{ij}$ describes the mutual interaction forces between adjacent blocks. The mathematical details are omitted here: the reader interested in this may refer to the works by Tinti *et al*. (1997, 1999), Bortolucci (2001) and Zaniboni (2004) for further details. Here we will just recall some

basic differences between the 1D and the 2D implementations of the approach. Concerning the partitioning of the sliding mass, in the 1D model the body is seen as a chain of blocks, while in the 2D model it is described as a matrix of blocks. Concerning the data that must be provided as input into the model, both implementations require information on the sliding surface relief and on the landslide geometry. Further, while in the 2D formulation the trajectory of the Com of each block is unknown a priori and is computed by the numerical code at each time step, in the 1D model the common path followed by the Coms and the side boundaries of the area swept by the slide on the sliding surface have to be prescribed a priori. One direct consequence is that, in the 1D case, the vector quantities in Eq. (1) can be substituted by scalars, since only the tangential components of acceleration, velocity and displacement along the common track of the Coms have to be computed.

The temporal variation of the local sea level that is determined by the underwater motion of the landslide is taken as the input for the tsunami simulation code, which implements and solves the non-linear non-dispersive Navier-Stokes equations in the shallow water approximation through a finite-element scheme. The equations implemented can be written as follows:

$$\partial_t \eta = \partial_t h_s - \nabla \cdot [(h + \eta)\, \vec{v}] \tag{2a}$$

$$\partial_t \vec{v} = g \nabla \eta - (\vec{v} \cdot \nabla \vec{v}) \tag{2b}$$

Eqs. (2a) and (2b) represent the continuity and momentum conservation equations, respectively: η is the water elevation above the still sea level, h the local sea depth, g the acceleration of gravity, $\vec{v}$ the depth-averaged horizontal velocity and h_s the instantaneous sea surface elevation determined by the underwater slide motion. Note that the term $\partial_t h_s$ in Eq. (2a) represents the connection between the landslide and the tsunami models. As regards the boundary conditions, we adopt a pure transmission condition for the water waves at the open sea boundaries, while on the coastal boundaries, treated as vertical walls, we impose a reflection condition where the "reflectivity", and hence the tsunami energy loss upon the coastal impact, can be tuned by varying a proper coefficient (see Tinti *et al*., 2005b for further details). We also account for a possible additional energy loss that is connected to the magnitude of the tangential component of velocity along the coastal boundary (see same reference as above).

3.2. Results

The main landslide of the first episode of mass failure was predominantly submarine. Accurate bathymetric surveys carried out in the shallow-water zone in front of the SdF (Chiocci *et al*., 2003a) revealed an evident underwater scar, deeper, close to the coast and gradually vanishing seaward, which was the total effect of the sequence of failures and of the possible secondary refilling of debris material. The estimated, corresponding missing volume exceeded 20×10^6 m^3. The volume (about 16×10^6 m^3) and the initial shape of the sliding body, assumed for numerical simulations, is in agreement with the survey outcome: it is about 700 m wide and 2200 m long (corresponding to an aspect ratio of about 1/3), with a top thickness larger than 30 m. The motion of the body was computed through the 2D landslide model for about 150 s until it reaches the water depth of around 1500 m: notice that the body is not at rest at the end of the simulation,

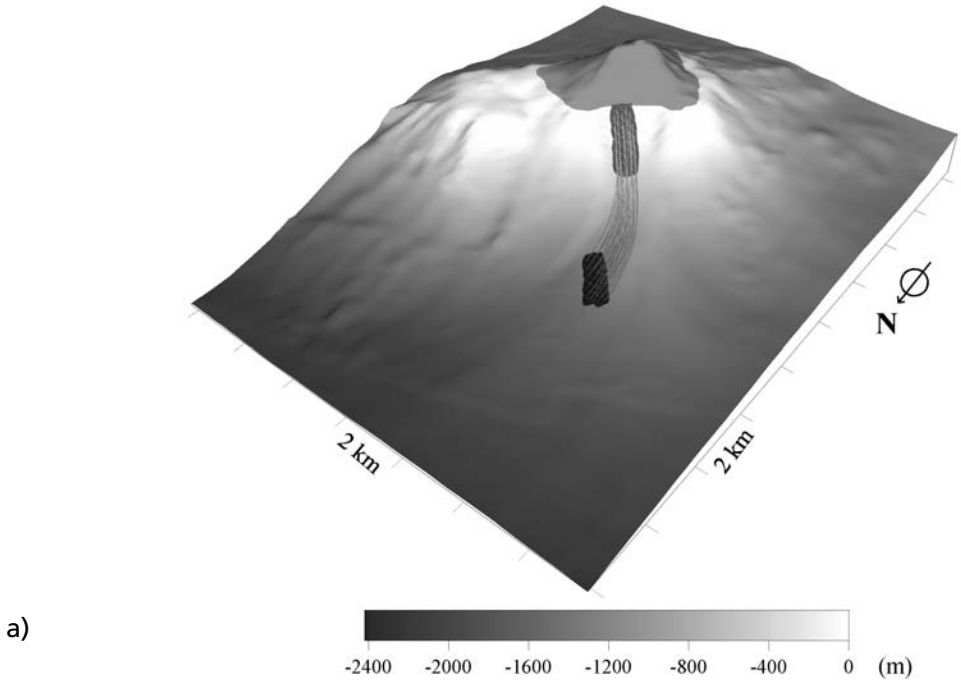

a)

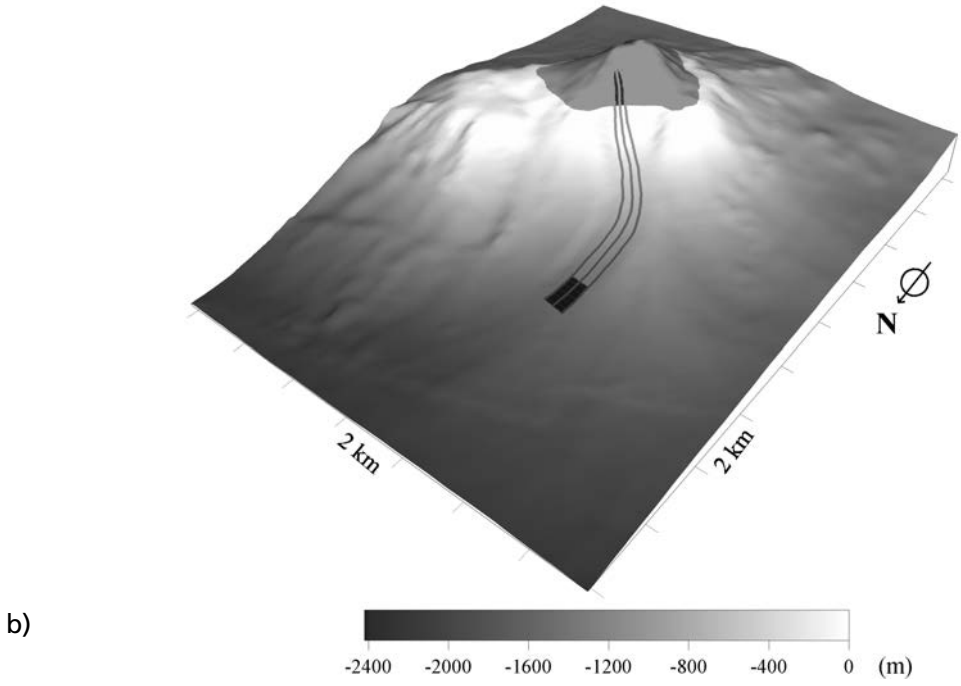

b)

Fig. 5 - a) Computed motion of the submarine landslide superimposed on the sea-bottom topography offshore SdF. The dynamics of this landslide, whose volume is in the order of 16×10^6 m^3, has been simulated through the 2D model, involving 32 blocks. The initial and final positions of the sliding mass are drawn respectively, as grey and dark-grey bodies, while the light-grey lines represent the trajectories of the com of the blocks. b) Initial and final position, together with the imposed sliding path, of the subaerial landslide detaching 7 minutes after the submarine one. This landslide, having a volume of 4.3×10^6 m^3, was simulated by means of the 1D model and was discretised into 10 blocks.

but since its tsunamigenic potential in deeper water is negligible, running the model more times is useless for tsunami generation studies. Fig. 5a portrays the initial position of the underwater mass and its position at the end of the simulation, together with the trajectories of the Com of the blocks where the landslide was partitioned. The slide moves within the old underwater scar produced in Holocene by the volcanic flank collapse originating SdF.

The second tsunamigenic failure was subaerial, and involved the uphill portion of SdF that was destabilised by the lack of mass at its foot, caused by the first sequence of failures. It took place about 7 minutes after the submarine sliding and was characterised by a series of detachments (Bonaccorso *et al*., 2003; La Rocca *et al*., 2004; Pino *et al*., 2004). The fresh scar on the flank of the mountain was clearly visible in the pictures taken on the December 31 by the survey team (INGV-CT) from helicopter flights over SdF (Bonaccorso *et al*., 2003): it was indeed composed of two distinct scars, a southern one (longer and deeper) and a northern one (smaller and narrower), separated by a large and dangerously unstable rock, that was progressively demolished in the later course of the volcanic eruption. Morphodynamic studies led to the conclusion that the southern scar was produced first (Chiocci *et al*., 2003b). Estimates of the total volume of the series of the subaerial slides of of December 30 can be made by using the results of aerial photogrammetric surveys and provide values around $8\text{-}10\times10^6$ m^3, but are corrupted by the intense dynamics of SdF in the days following these main episodes, which includes both massive lava flows (that partly refilled the scar) and progressive fracturing, fragmentation and collapsing of unstable masses (see Baldi *et al*., 2003; Chiocci *et al*., 2003b).

In this study, we assume that the first landslide of the subaerial sequence was the one that left the southern scar, that it generated the second tsunami, and that it moved about one half of the total estimated volume, involving slightly more than 4×10^6 m^3 of material. The slide, that was quite narrow with an average width of about 150 m and was slightly longer than 1 km (equivalent to an aspect ratio smaller than 1/6), was modelled by means of the 1D code, and the necessary input data (i.e. common path of the Com of the blocks and side boundaries of the area swept by the moving slide) were prescribed on the basis of the results obtained for the submarine landslide studied through the 2D model. Fig. 5b shows the initial and final positions of the subaerial slide. Calculations were stopped when the body was at around 1500 m depth, as in the previous case, for the same reasons.

The tsunamis generated by the landslides were analysed by means of the tsunami simulation model highlighted in the section before. Here the interest is focussed on the impact of the waves on the northern and north-eastern coasts of Stromboli that happened to be the most affected by the tsunamis. To this purpose, the finite-element grid built to run the model is a high-resolution mesh along the coast with average inter-nodal distance around 20-30 m. Figs. 6 to 9 display a series of water elevation time-histories computed at as many as 25 coastal nodes in the belt running from south of Pizzillo to west of Ficogrande that is portrayed in the map blow-up of Fig. 1c. The calculated records show the wave motion induced by the first tsunami (solid line) as well as the waves produced by the combination of the first and of the second tsunami (dotted line). The instant when the two lines depart from each other is exactly when the second tsunami attacks the coastal site. The delay between the two is assumed to be 7 minutes at the source, consistently with the time separation of the landslide seismic signals (La Rocca *et al*., 2004; Pino *et al*., 2004) and it is approximately, but not exactly the same, at all coastal points. The reason for

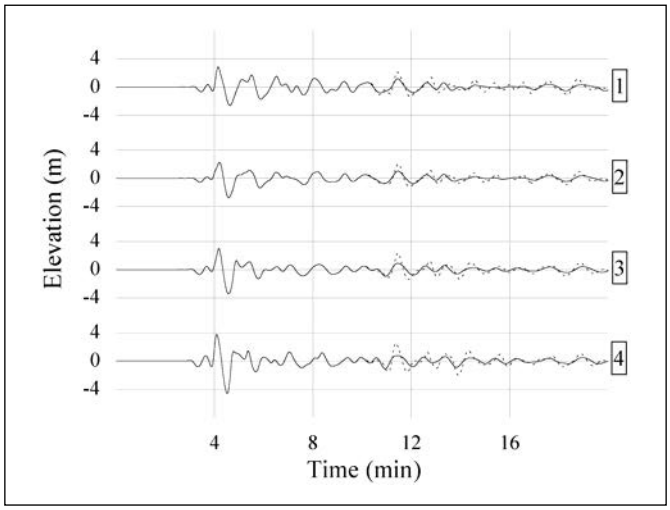

Fig. 6 - Tsunami records computed around the wharf of Pizzillo.

the slight difference in arrival times in the various sites resides in the fact that the propagation speed of non-linear waves depends not only on the bathymetric features, but also on the wave amplitude and sign: for example, troughs are known to travel slower than crests in shallow-water. The leading wave of the first tsunami is everywhere a trough, which is consistent with most eye-witness observations (Tinti *et al*., 2005a) and with the source mechanism. Indeed, the fact that the tsunami arrival was a sea retreat was one of the first pieces of evidence acquired during the first post-disaster hours and oriented the search for a submarine mass failure that was actually identified some days later. On the other hand, the modelled leading wave of the second tsunami is a small crest, as the result of the subaerial slide impact on the sea water. Consequently, the two tsunamis have fronts of opposite sign and travel with slightly different speeds, the second being the faster one.

Fig. 6 shows the synthetic tide-gauge record around Pizzillo (Fig. 1c), that is the wharf of Stromboli, where all private boats and all ferries carrying goods and passengers dock. Among the places selected for this study, it is the most distant from the source. The tsunami attacks this area with a small oscillation first, and then with a large wave ranging from a 3-4 m amplitude about 4 minutes after the beginning of the tsunami (which is the origin time in all the marigram graphs). The second tsunami is small here and can be confused with the queue of the first. From eye-witness accounts, we know that the inundation here was only minor and tsunami damage was light (Tinti *et al*., 2005a). Therefore, our computations probably overestimate the height of the wave.

Fig. 7 regards the area called Scari: it is a long low beach, of small pebbles and stones, with a road running parallel to the sea, which is one of the two main connections between the harbour area (Pizzillo) and the hamlets of the northern coast. A harbour office (on the seaside of the road) and the island electric power plant (on the other side) are located here. Measured run-up heights taken during the surveys provide values from 3 up to over 5 m (Tinti *et al*., 2005b). At the selected nodes, the computed tsunami has maximum amplitude around 4 m in the south (nodes 5-7) and

around 3 m in the north (nodes 8-10), which is in substantial agreement with observations. Notice that the arrival of the second tsunami wave train is well distinguishable here from the queue of the first.

Fig. 8 covers the area of Punta Lena. Please observe that this is the same name for two different places in Stromboli: the one treated here that is the north-eastern "corner" of the island, and the one forming the south-eastern "corner", the latter being practically uninhabited. Punta Lena is a residential place with a number of new and restored holiday houses aligned along the waterfront that were all severely affected or destroyed by the impact of the waves. Measured run-up heights grow westwards and fall between 3 and more than 7 m (Tinti *et al*., 2005b). Here, both the first and the second modelled group of waves are rather high and powerful, with maximum amplitudes lying around or above 4 m in all the time-histories given in Fig. 8. The maximum calculated water elevation exceeded 8 m, at the coastal nodes of the grid belonging to this area.

Fig. 9 refers to Ficogrande, a tourist resort with hotels, restaurants and shops aligned along the promenade on the side opposite side of the beach. To the east, Ficogrande begins where an old pier protruding almost normally to the coastline and that is now no longer used. In most places here, run-up heights exceeded 5 m and values over 9 m were measured in the easternmost part of Ficogrande (Tinti *et al*., 2005b). The tide-gauge records depicted in Fig. 9 show maximum water elevation around 5 m for all the selected points and in excess of 8 and 9 m in some points (nodes 19 and 20), which agrees well with observations. Notice also that the second tsunami waves stand out quite clearly from the queue of the first tsunami, and are very large (nodes 18-20), though smaller than the ones of the first attacking train.

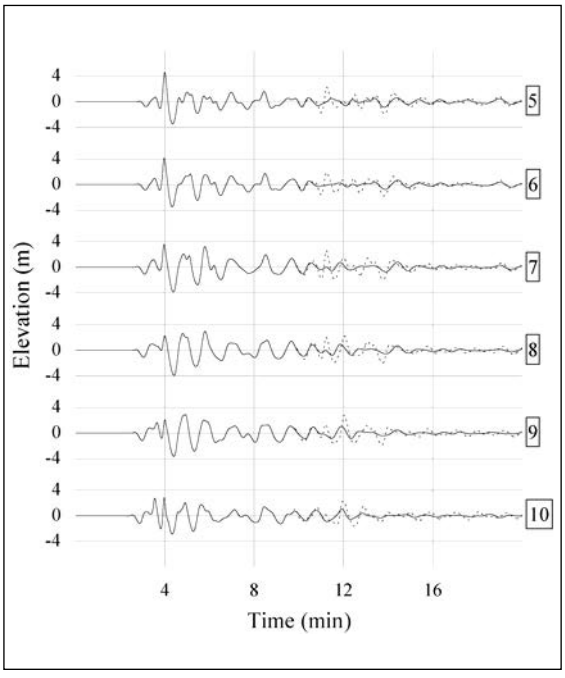

Fig. 7 - Tsunami tide-gauge records calculated at Scari, that is the longest and the widest beach of Stromboli.

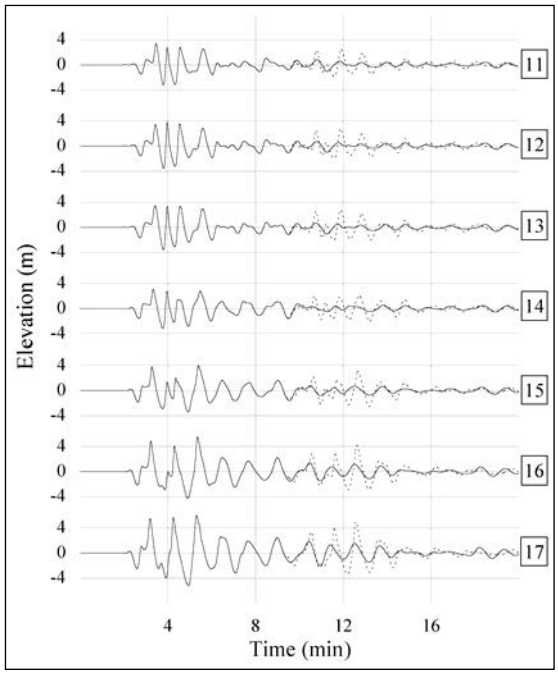

Fig. 8 - Time-histories calculated around Punta Lena, the north-eastern corner of the Island of Stromboli.

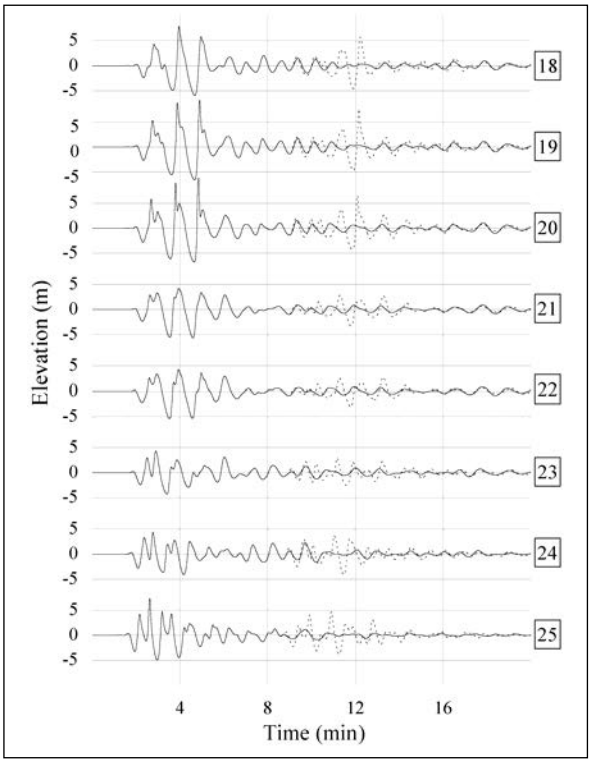

Fig. 9 - Marigrams computed at the beach of Ficogrande (18-22) and on the stretch of coast to the west of it, formed by protruding rocks and small creeks.

Fig. 10 is a zoom of the area of Ficogrande and of the coast to the west of it. The largest (crests) and smallest (troughs) values of water elevation computed for marigrams from nodes 18-25 are used here to estimate the corresponding maximum penetration of the sea water onshore as well as the maximum withdrawal from the shoreline. This is obtained by making use of accurate bathymetric data and of a high-resolution digital terrain model provided respectively by Prof. Vettore (University of Padova) and by Prof. Baldi (University of Bologna). The inundation values (crosses) are checked against the observed inundation line (white line) that was obtained by field surveys performed by several research teams (see e.g. Tinti *et al*., 2005b) and by local teams under the direct supervision of the Civil Protection authorities. The withdrawal line cannot be checked against quantitative data. The only piece of information available for this area that provides clues on the amount of the sea retreat comes from the account of Mr. Nino Zaccone, a resident of Stromboli. At the instant of the first tsunami attack, he was driving along the road from Ficogrande heading to Pizzillo. He did not notice the first sea recession since he was looking ahead in the direction opposite from where the tsunami was coming. He was dramatically alerted by other people who happened to be riding scooters on the same road and saw the tsunami arriving. Luckily, the whole group of people managed to escape to higher ground and were not carried away by the waves. A detailed analysis of the reports of the tsunami eye-witnesses in Ficogrande and in other places of Stromboli may be found in Tinti *et al*. (2005a). It is of special interest here to point out a detail, that was omitted there, concerning Mr. Zaccone. From his safer observation point he was able to see the evolution of the tsunami wave and later reported:

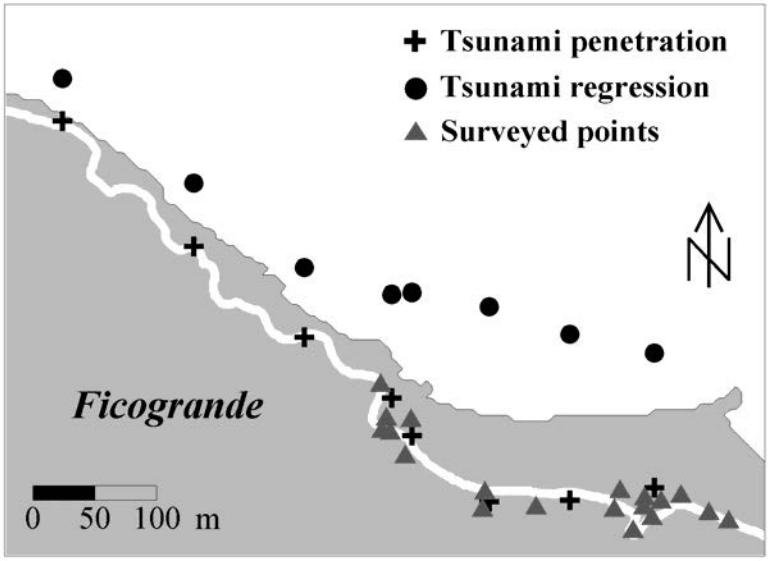

Fig. 10 - Maximum penetration (crosses) and maximum regression (solid circles) evaluated in 8 sites located at and to the west of Ficogrande. The observed maximum penetration is marked by the thick white line. Dark-grey triangles show the points where the measurements of the tsunami run-up were taken during the post-event surveys.

"*…I heard a loud noise, such as the one of stones rolling down. The wave was going back (seawards) and I saw the bottom of the sea uncovered. The depth was around 6 m. I know it, because the water uncovered the old iron-pier that lies underwater in front of the Hotel La Sirenetta and that was used once by the hydrofoils. In my mind the water amplitude was about 7 m…*". Node 20 (Fig. 1c) is the closest to the Hotel La Sirenetta in the node selection considered here. The related tide-gauge record is given in Fig. 9 and shows a water depression larger than 5 m for the second and third water oscillations. This agrees quite satisfactorily with Mr. Zaccone's account and, correspondingly, gives confidence on the estimated water retreat in this area.

4. Conclusions

This work is a numerical reconstruction of the landslides and of the corresponding tsunamis that affected Stromboli and the neighbouring islands on December 30, 2002. The study complements a previous analysis (Tinti *et al*., 2005c) that reported on a number of landslides and tsunami simulations that were carried out with the purpose of identifying the most plausible sources and source mechanisms of the tsunamis. Here, we focus only on the cases that were found to represent the sources best: a submarine landslide of about 16×10^6 m^3 detaching from just below the sea surface level in the north SdF area that was responsible for the first tsunami, and a subaerial slide, about one third of the former, that detached as the result of the retrogressive migration of the instability, 7 minutes later. The main interest here is focussed on the behaviour of the tsunamis on the coasts of Stromboli that were found to be the most affected by the impact of the water waves. The work presents a series of synthetic tide-gauge records computed at a

selection of 25 coastal points, extracted from the high-resolution finite-element mesh that was used for tsunami simulation.

It is found that the agreement between the computed waves and the observations is remarkably good. In particular, the issues that match favourably can be summarised as follows.

1) The computed maximum water heights to the west of and at Ficogrande, and in the area of Punta Lena, agree with the measured run-up heights. Matching is also satisfactory at Scari beach.
2) The largest water wave is not the first one, but the second or the third one, and this is in accordance with reports of most eye-witnesses.
3) The first tsunami arrival is a negative water oscillation corresponding to a sea retreat, as observed by almost everybody.
4) In some places the second tsunami is rather indistinguishable from the queue of oscillations of the first tsunami series, while at other sites the second train is well above the mean amplitude of the queue. This is consistent with the fact that only few eye-witnesses recognised the occurrence of two distinct tsunamis, while most believed they saw only one.
5) The maximum water recession and penetration estimated by means of our modelling in the area of Ficogrande, agree with the onshore observations and the eye-witness reports.

In addition to the above items, some points of weakness that call for modelling refinement could be identified.

1) The maximum water heights calculated around Pizzillo are higher than the observations.
2) The first water withdrawal calculated at Pizzillo is probably too weak. Here an eye-witness noticed a strange long ebb tide preceding the arrival of the tsunami (see Tinti *et al*., 2005a).
3) The computed second tsunami is probably too weak, especially at Punta Lena. The attack of the second tsunami was shot in a series of pictures by Mr. Utano, a resident of Stromboli, from a panoramic viewpoint placed in the hamlet of San Vincenzo (Tinti *et al*., 2005a). From his photos, we know that Punta Lena was attacked by a high wall of water (a breaking wave), whose height is yet difficult to evaluate, but is likely larger than the one calculated here.
4) The above uncertainties around the second tsunami are paralleled by the uncertainty on its source. The assumption on the volume made here (4.3×10^6 m^3) may not be too far from the truth, but the available constraints are quite weak. Indeed the main uncertainty resides in the total volume of the mass missing from the a.s.l. western flank of Stromboli, since the effusive eruption activity and the related mass instabilities, that continued for a long time after the main episode of failures, spoiled the theatre, and perhaps made it prohibitive to perform a correct estimation of the involved volume through aerophotogrammetry.

In the light of the above remarks, future research will concentrate on ways of better determining the second source and on a more sophisticated modelling of the second landslide. Further improvements are expected from using a finer numerical mesh especially for tsunami simulations in the area of Pizzillo.

Acknowledgements. This paper was presented at the 22nd Convegno Nazionale GNGTS, Rome, 18-20 November 2003 and was funded through an INGV-GNV grant in the framework of an agreement with the Italian Civil Protection. We thank Professor Paolo Baldi (Dipartimento di Fisica, Università di Bologna) and his group for providing us with the DTM of the Island of Stromboli. We are also indebted to Professor

Antonio Vettore and his group (Dipartimento Territorio e Sistemi Agro-Forestali, Università di Padova) for supplying us with the high-resolution bathymetry acquired around the shallow-water coastal belt of Stromboli in the framework of the INGV-GNV Project "Pericolosità del Vulcano Stromboli" co-ordinated by Professor Mauro Rosi. We are extremely grateful to Professor Bernardo De Bernardinis, General Director of the Office of Prevision and Prevention of the Italian Civil Protection, Rome, who authorised the acquisition of field data during the emergency and provided us with all the needed technical and logistical assistance and support.

REFERENCES

Baldi P., Belloli F., Fabris M., Marsella M., Monticelli R. and Signoretto V.; 2003: *La fotogrammetria digitale differenziale del versante della Sciara del Fuoco (isola di Stromboli) dopo l'evento del 30 dicembre 2002.* 7ª Conferenza Nazionale ASITA "L'informazione territoriale e la dimensione del tempo", Verona, 28-31 ottobre 2003 (in Italian).

Bonaccorso A., Calvari S., Garfì G., Lodato L. and Patanè D.; 2003: *Dynamics of the December 2002 flank failure and tsunami at Stromboli volcano inferred by volcanological and geophysical observations.* Geophys. Res. Lett., **30**, 1941, doi: 10.1029/2003GL017702.

Bortolucci E.; 2001: *Modelli dinamici di frane e dei maremoti indotti*. Tesi di Dottorato di Ricerca in Fisica, XIV Ciclo, Anno Accademico 2000-2001, Università di Bologna, 126 pp. (in Italian).

Chiocci F.L., Bosman A., Romagnoli C., Tommasi P. and de Alteris G.; 2003a: *The December 2002 Sciara del fuoco (Stromboli island) submarine landslide: a first characterisation*. EGS-AGU-EUG Joint Assembly, Nice, France, April 2003, Geophysical Research Abstracts, Vol. 5, CDROM version.

Chiocci F.L., Coltelli M., Marsella M., Pompilio M. and Tommasi P.; 2003b: *Analysis of the first data on the instability phenomena associated to the 2002-2003 "Sciara del Fuoco" (Stromboli, Italy) lava flow eruption in the perspective of preliminary risk evaluation*. EGS-AGU-EUG Joint Assembly, Nice, France, April 2003, Geophysical Research Abstracts, Vol. 5, CDROM version.

La Rocca M., Galluzzo D., Saccorotti G., Tinti S., Cimini G. B. and Del Pezzo E.; 2004: *Seismic signals associated with landslides and with a tsunami at Stromboli volcano, Italy*, Bull. Seism. Soc. Am., **94**, 1850-1867.

Maramai A., Graziani L. and Tinti S.; 2005: *Tsunamis at the Aeolian islands (southern Italy): a review*. Marine Geology, **215**, 11-21.

Pino N.A., Ripepe M. and Cimini G.B.; 2004: *The Stromboli Volcano landslides of December 2002: A seismological description.* Geophys. Res. Lett., **31**, L02605, doi: 10.1029/2003GL018385.

Tibaldi A.; 2001: *Multiple sector collapses at Stromboli volcano, Italy: How they work.* Bull. Volcanol., **63**, 112-125.

Tinti S., Bortolucci E. and Romagnoli C.; 2000: *Computer simulations of tsunamis due to flank collapse at Stromboli, Italy.* J. Volcanol. Geoth. Res., **96**, 103-128.

Tinti S., Bortolucci E. and Vannini C.; 1997: *A block-based theoretical model suited to gravitational sliding*. Natural Hazards, **16**, 1-28.

Tinti S., Bortolucci E. and Armigliato A.; 1999: *Numerical simulation of the landslide-induced tsunami of 1988 in Vulcano island, Italy*. Bull. Volcanol., **61**, 121-137.

Tinti S., Manucci A., Pagnoni G., Armigliato A. and Zaniboni F.; 2005a: *The 30th December 2002 tsunami in Stromboli: sequence of the events reconstructed from the eyewitness accounts*. Bull. Volcanol. (submitted).

Tinti S., Maramai A. and Graziani L.; 2004: *The new catalogue of Italian tsunamis*. Natural Hazards, **33**, 429-465.

Tinti S., Maramai A., Armigliato A., Graziani L., Manucci A., Pagnoni G. and Zaniboni F.; 2005b: *Quantitative observations of the physical effects of the Stromboli tsunamis occurred on December 30th, 2002*. Bull. Volcanol. (under revision).

Tinti S., Pagnoni G., Zaniboni F. and Bortolucci E.; 2003: *Tsunami generation in Stromboli island and impact on the south-east Tyrrhenian coasts.* Nat. Hazards Earth Sys. Sci., **3**, 1-11.

Tinti S., Pagnoni G., and Zaniboni F.; 2005: *The landslides and tsunamis of 30th December 2002 in Stromboli analysed through numerical simulations*. Bull. Volcanol. (accepted for publication).

Tinti S. and Vannini C.; 1995: *Tsunami trapping near circular islands*. Pure Applied Geophys., **144**, 595-619.

Zaniboni F.; 2004: *Modelli numerici di evoluzione di frane con applicazione a casi di frane tsunamigeniche subaeree e sottomarine*, Tesi di Dottorato di Ricerca in Modellistica Fisica per la Protezione dell'Ambiente, XVI Ciclo, Anno Accademico 2003-2004, Università di Bologna, 112 pp. (in Italian).

Corresponding author: Stefano Tinti
Dipartimento di Fisica, Settore di Geofisica, Università degli Studi di Bologna
Viale Carlo Berti Pichat 8, 40127 Bologna, Italy
phone: +39 051 2095025; fax: +39 051 2095058; e-mail: steve@ibogfs.df.unibo.it